Automatika

Journal for Control, Measurement, Electronics, Computing and Communications

ISSN: (Print) (Online) Journal homepage: https://www.tandfonline.com/loi/taut20

An efficient SLM technique based on chaotic biogeography-based optimization algorithm for PAPR reduction in GFDM waveform

S. Selvin Pradeep Kumar, C. Agees Kumar & R. Jemila Rose

To cite this article: S. Selvin Pradeep Kumar, C. Agees Kumar & R. Jemila Rose (2023) An efficient SLM technique based on chaotic biogeography-based optimization algorithm for PAPR reduction in GFDM waveform, Automatika, 64:1, 93-103, DOI: 10.1080/00051144.2022.2106532

To link to this article: https://doi.org/10.1080/00051144.2022.2106532

Published online: 07 Aug 2022.

AUTOMATIKA
2023, VOL. 64, NO. 1, 93–103
https://doi.org/10.1080/00051144.2022.2106532

REGULAR PAPER

OPEN ACCESS Check for updates

An efficient SLM technique based on chaotic biogeography-based optimization algorithm for PAPR reduction in GFDM waveform

S. Selvin Pradeep Kumar[a], C. Agees Kumar[b] and R. Jemila Rose[c]

[a]Department of Electronics and communication Engineering, St. Xavier's Catholic College of Engineering, Chunkankadai, India; [b]Department of Electrical and Electronics Engineering, Arunachala College of Engineering for Women, Vellichanthai, India; [c]Department of Computer Science and Engineering, St Xavier's Catholic College of Engineering, Chunkankadai, India

ABSTRACT

High data rates, extremely low power consumption, and minimal end-to-end latency are considered to be mandatory requirements for 5G wireless networks. Rapid improvements in design and performance of 5G physical layer waveforms have become necessary. The drawback of Orthogonal Frequency Division Multiplexing (OFDM) is high PAPR, that causes signal distortion, which reduces system efficiency. Generalized frequency division multiplexing (GFDM) is a promising non-orthogonal multicarrier transmission scheme, which has recently received a great deal of attention towards future fifth generation (5G) wireless networks. It overcomes the limitations of orthogonal frequency division multiplexing (OFDM), while preserving most of the advantages of it. Selective Level mapping (SLM) is one of the PAPR reduction techniques, that uses the phase shift technology. In this paper, SLM based on Chaotic Biogeography Based Optimization (CBBO) algorithm is proposed to offer an efficient solution to the problem of high PAPR, existing in the GFDM waveforms. Experimental results prove that, the proposed CBBO–SLM technique provides significant improvement in terms of PAPR reduction, as compared to the conventional SLM methods, such as conventional GFDM and OFDM-SLM. The proposed novel scheme is most suitable for QAM and QPSK applications, as it provides good PAPR reduction performance, at lower computational complexity.

ARTICLE HISTORY
Received 11 September 2021
Accepted 21 July 2022

KEYWORDS
Generalized frequency division multiplexing; selective level mapping; peak to average power ratio; chaotic biogeography based optimization

1. Introduction

The fast development of mobile communication enables quick innovation in terms of new applications and venture formation due to its broad coverage and robust ecosystem. The impending fifth generation (5G) of mobile networks is projected to provide new chances to sustain long-term profitability in the era of the Internet of Things (IoT), autonomous driving, and augmented and virtual reality (AR/VR) services. 5G cellular architecture and associated air interface improvements [1] are currently being developed, with 75 billion projected by 2025 [2] to support large deployments of connected devices. 5G is not just a step up from past generations of cellular technology; it's a game-changing technology that promises to break through barriers to global connectivity in terms of access, bandwidth, performance, and latency. 5G services have the ability to significantly improve global quality of life through facilitating software advancements, sectors, and business models. Through extraordinary use cases for new mobile, e-Health, electric cars, smart buildings, and home automation are examples of applications that require high data rates, low latency, and a large number of connections, 5G networks, in contrast to current 4G networks, offer new wireless interfaces that support higher frequencies and spectrum efficiency.

As an air interface technique, several wireless protocols include Orthogonal Frequency Division Multiplexing (OFDM) [3]. DAB (digital audio broadcasting), DVBT (digital video broadcasting for terrestrial television), WLAN (802.11family), and 4G cellular technologies are all examples (LTE-A). OFDM has several advantages, including low complexity equalization, which makes it immune to inter-symbolic interference (ISI). This is accomplished through the use of a Cyclic Prefix (CP) and Frequency Domain Equalization (FDE). The efficient use of IFFT/FFT processing reduces the Waveform processing. Seyye Hadi et al. [4] proposed the greedy deterministic algorithms based on the OFDM system. In this technique, they optimize the value with the help of pilot. The pilot are references signal to use in transmit and receive side.

In this algorithm, to solve the optimization problem (e.g. AdHoc WSN) use three algorithm and they define the properties and compare the all channel. In addition, when the distances of both pilots are multiple integrals, a minimum distance term is introduced, resulting in a short runtime and minimal complexity. It

CONTACT S. Selvin Pradeep Kumar selvin.s.pradeepkumar@gmail.com Department of Electronics and communication Engineering, St. Xavier's Catholic College of Engineering, Chunkankadai, Tamil Nadu, India

recovers all problems with the help of channel estimation methods. The three algorithms are used in OFDM and compare the BER and SNR. Jung-Chieh, Chen et al. [5] identified the main problem of OFDM with sparse channel estimation in a pilot. To reduce the complexity and increases the accuracy with OFDM system and also increase the spectral efficiency. In a simulation result, the pilot are using an OFDM to provide better performance as compared to the other computational method like equi-spaced scheme and random method.

OFDM is a modulation technique for the latest version of 4G wireless communication system in high bit rate transmission system. The bandwidth is precious and it provides a more number of users in channel estimation. Channel estimation plays an important part in an OFDM system. It is used for increasing the capacity of orthogonal frequency division multiple access (OFDMA) systems by improving the system performance in terms of bit error rate. Osvaldo et al. 2004 [6] Proposed the pilot is based on channel estimation for OFDM system. Because OFDM systems use a rapid fading channel, channel estimation and tracking is done by broadcasting a signal that contains known pilot symbols in specific places.

When compared to other qualities, several researchers propose improvements to the OFDM waveform to reduce spectrum contamination and sensitivity to carrier frequency offset. Recently GFDM, FBMC [7], UFMC [8], and BFDM [9] have been proposed to replace OFDM. Advancements and replacements to the OFDM waveform have been presented in recent research. The objective is to create a waveform that is simple to broadcast and receive, resistant to frequency offset and hardware flaws, has adequate time and frequency localization, and can be easily updated to meet 5G requirements by adding MIMO signal processing.

The paper's main contributions can be summarized as follows:

- Novel SLM-based technology termed CBBO–SLM was established and used in the GFDM system.
- This novel CBBO based SLM algorithm has been used to reduce the PAPR at lowest level compared to the existing technique.

The following is how this paper is organized: The first section introduces the recommended flow, while the second section explains the relevant tasks. Section 3 defines the intended work. The CBBO-based SLM and the chaotic BBO algorithm are discussed in this section. Section 4 analyses the simulation findings before presenting the conclusions in Section 5.

2. Related works

GFDM is a non-orthogonal multi-carrier modulation method made up of a number of subcarriers, each of which comprises sub symbols produced over many time intervals. A prototype circular convolution filter is used to pulse-shape the subcarriers independently. The amount of subcarriers and sub symbols, as well as the degrees of freedom assessed by the prototype filter, determine GFDM flexibility. The OOB emissions of GFDM decrease as a result of using a pulse shaping filter, making it suitable for noncontiguous frequency bands. The GFDM synchronization limitations could also be reduced by employing an additional cyclic suffix.

Rosas et al. (2015) [10] established a power allocation technique for two different multicarrier systems, OFDM and GFDM, using the Genetic Algorithm. This method seeks the greatest power value for each subcarrier in order to maximize the overall downlink CR network throughput of the SUs. The GFDM system outperforms the OFDM system in terms of SUs. Panaitopol et al. (2012) [11] examine and assess the sensing properties of the GFDM system using cyclo-stationarity features. Matthe et al. (2015) [12] established a technique for achieving transmit diversity with a GFDM system by using Widely Linear Estimation (WLE) to decrease the impact of the ISI. To optimize overall throughput for the SUs while remaining within maximum power and interference limitations for cognition, an efficient power allocation method based on the PS algorithm is utilized.

Zewail et al. (2016) investigated the GFDM system [13]. To optimize the SU's data rate while preserving the Access Point's maximum transmitted power and the PUs' threshold interference, the PS method is applied to find the best power level for each sub-channel. Bitnerr et al. [14] provide a more efficient method for OOB emission as well as PAPR reduction. Sim et al. [15] use a Quadratic Programming methodology to create a practical pulse shaping filter that reduces the PAPR. According to numerical simulations, the proposed pulse shaping filter reduces the PAPR by roughly 3 dB. The impact of HPA nonlinearity on GFDM systems is investigated by Jayati et al. [16]. In this study, the Rapp model is utilized to model the HPA type Solid State Power Amplifier (SSPA).

Based on the filter bank idea the GFDM modulation as a multicarrier modulation was initially developed [17]. The matrix model for the GFDM transmitter was constructed in linear form in [18]. Furthermore, the BER and OOB emission of GFDM, as well as the effects of pulse shaping on GFDM performance, were investigated using various prototype filters [19,20] examined GFDM's adaptation to 5G networks by looking at a number of its features. Although GFDM appears to be a reasonable candidate for 5G, it has a restricted practical implementation. One is that it is more complex than OFDM, which is a major disadvantage. As a result, the receiver's complexity was reduced by modelling GFDM in frequency domain and leveraging the sparse feature of the filter in [21].

Furthermore, [21] recently demonstrated a low-cost modem structure based on the rapid Fourier transform (FFT). For the air interface of 5G networks, a flexible multicarrier modulation technique has also been suggested [22]. GFDM's flexibility allows it to be utilized for CP-OFDM and single carrier frequency domain equalization (SC-FDE).

To reduce the high PAPR in GFDM systems, two PAPR reduction methods have been proposed: clipping [23] and precoding [24,25]. While clipping reduces PAPR, it also causes distortion and reduces bit error rate (BER) performance. The Walsh-Hadamard transform was employed in the precoding approach in [26], which resulted in a 2.5-dB PAPR decrease. Filtering is used to transport data symbols to the appropriate time slot and frequency range, allowing the data block to be split into many subcarriers and sub symbols. Using pulse shaping techniques, the PAPR was lowered by about 2 dB [27–29].

In practice, these ideal pulse shaping filters, on the other hand, are non-causal and unattainable, truncation is required to execute the ideal pulses, which causes frequency domain distortion. Jeyanti and Shipan [30] devised a novel hybrid Particle Swarm Optimization–Pattern Search Algorithm (PSO–PS). It has been successfully utilized to determine the best power value for each subcarrier in order to maximize total throughput.

The quantity of formed candidate signals exceeds the amount of phase sequences generated randomly in this SLM process. In terms of PAPR reduction capabilities, simulated testing shows that the related approach beats the standard SLM [31]. Pamungkasari et al. examine [32] the performance of the low complexity time domain cyclic SLM (TD-C-SLM) in MIMO-OFDM systems. TD-C-SLM generates the signal candidates by summing the original OFDM signal another work done by Pamungkasari et al. [33] proposed the effects of cyclic shift resolution of the OFDM system with C-SLM-DC-MF scheme on the system performance, in terms of PAPR reduction, accuracy, and bit error rate (BER). Prasad and Ramesh [34] analyzed various phase sequences such as Riemann, Centering, Centred Riemann and New Centred to Modified SLM technique and their effect on PAPR reduction. Valluri and Mani [35] utilized the concepts of conversion matrices and linearity to achieve low complexity with respect to the modulation matrices in the conventional SLM method. This paper [36] introduces a novel sort of companding transform for decreasing the PAPR of UFMC signals. SLM's computational complexity reaches extremely high levels when using this method. Conventional SLM technique has relatively high complexity due to the use of some inverse discrete Fourier transform (IDFT) operations. In addition, it requires transmitting side information (SI) to the receiver. To avoid this undesirable condition, appropriate solutions must be found with the smallest amount of searches possible. For lowering PAPR in the GFDM system, a novel approach named Chaotic Biogeography Based Optimization based SLM (CBBO–SLM) was created.

3. Proposed work

The goal of this study is to develop CBBO-based SLM methods for PAPR reduction. CBBO-based phase optimization is used to identify effective choices with fewer search numbers rather than producing a large number of random phase sequences. To optimize phase sequences, the CBBO method employs the SLM algorithm. SLM technique stands out as one of the most preferred PAPR reduction algorithms due to its both easy to use structure and efficient, that is useful for finding effective solutions in discrete space.

(a) GFDM transmitter

The first phase in the GFDM transmitter is the QAM mapping of the information bits. The corresponding approach divides the whole band into several sub-bands, some of which are assigned a set of QAM patterns.

$$X_b(k) = \begin{cases} X(K), & \text{if } (b-1)(N/B) \le k \le b(N/B) - 1 \\ 0 & \text{otherwise} \end{cases} \tag{1}$$

$K = 0, 1, 2, \ldots, N-1;\ b = 1, 2, 3, \ldots, B.$

The symbol sequence is specified by $X(K)$, and the frequency domain data of the sub-band b is represented by $X_b(k)$. N and B stand for the number of subcarriers and sub-bands, respectively, while k stands for the subcarrier indices. Following that, each sub-band is subjected to the inverse fast Fourier transforms (IFFT) procedure [22].

$$X_b(n) = \frac{1}{\sqrt{N}} \sum_{k=0}^{N-1} X_b(k) e^{\frac{j2\pi kn}{N}}, \quad 0 \le n \le N-1;\ 1 \le b \le B \tag{2}$$

Figure 1 shows the advancement of the GFDM system transceiver. To create an encoded data vector ($\vec{b}_c$), the data source first sends a data vector ($\vec{b}$) to the encoder. A signal mapper translates groups of encoded bits into symbols, where is the number of bits per symbol in the modulation scheme. Figure 3 depicts the progress of the GFDM system modulation. The resulting vector ($\vec{d}$) represents a specific block with N symbols separated into M sub-symbols and K sub-carriers.

$$\vec{d} = (\vec{d}_0^T, \ldots\ldots\ldots\ldots, \vec{d}_{M-1}^T)^T \tag{3}$$

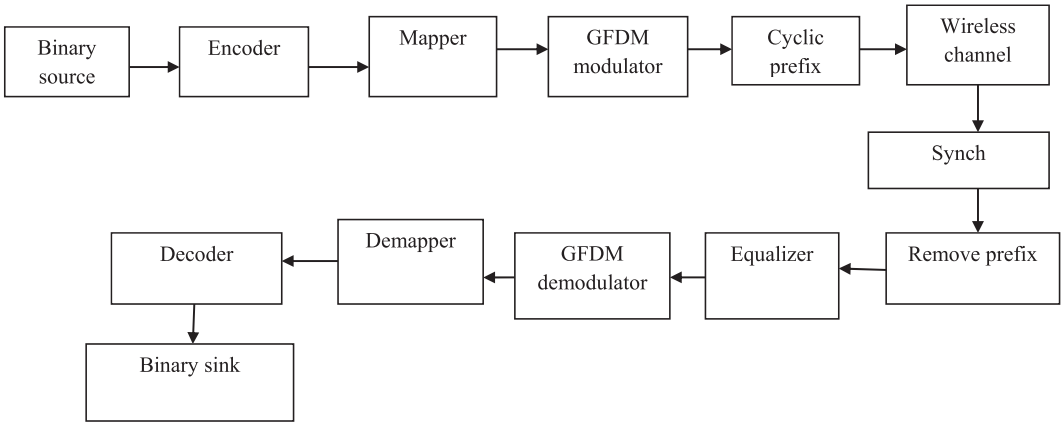

Figure 1. Diagram of GFDM system transceiver.

where

$$d_m = (d_{0,m}, \ldots\ldots\ldots, d_{k-1,m})^T \tag{4}$$

Each individual symbol $d_{k,m}$ indicates the data symbol that will be sent on the GFDM block's k^{th} sub-carrier and m^{th} sub-symbol. Each symbol ($d_{k,m}$) is filtered with the pulse shape that it corresponds to, as described by (4).

$$g_{k,m}[n] = g[(n - mk) \bmod N]e^{-j2\pi \frac{k}{k}n} \tag{5}$$

Where the sampling index is indicated as n and $g_{k,m}$ is the time and frequency shift of the prototype filter's. The transmit samples that arise can be represented as

$$x[n] = \sum_{k=0}^{k-1} \sum_{m=0}^{m-1} g_{k,m}[n] d_{k,m} \tag{6}$$

where $n = 0, \ldots, N-1$. It's possible to rewrite the previous equation as

$$\vec{x} = A\vec{d} \tag{7}$$

where A is the source matrix, which has size of KM × KM and is defined by

$$[\overrightarrow{g_{0,0}} \cdots\cdots \overrightarrow{g_{k-1,0}} \overrightarrow{g_{0,1}} \cdots\cdots\cdots \overrightarrow{g_{k-1,m-1}}] \tag{8}$$

(b) Channel

The wireless channel impulse response h[n] should be equal to or less than the channel length. At the receiver, precise synchronization and channel status information are also expected. The received waveform may be represented as after removing the CP.

$$y[n] = x[n] \circledast h[n] + w[n] \tag{9}$$

where $w[n]$ denotes the AWGN with zero mean and σ^2 variance, and $\circledast$ refers to circular convolution with respect to n and periodicity N. After that, the frequency domain equalization is done as follows:

$$\hat{x}(n) = F^{-1}\left[\frac{F(y[n])}{F([h/n])}\right] \tag{10}$$

where F – the Discrete Fourier Transform.

(c) GFDM Receiver

The receiver demodulation can be expresses as

$$\hat{d} = B.\hat{x} \tag{11}$$

The demodulation matrix is denoted by B.

$$B = A^{-1} \tag{12}$$

The PAPR at the GFDM system's transmitter needs to be reduced. Because a large linear dynamic range in the radio frequency power amplifier (RFPA) is required for a high PAPR. If this is not done, the launch signal will easily enter the nonlinear area, resulting in sounds that will increase system error and performance loss. However, increasing the linear range reduces device efficiency and raises the expense of practical engineering due to the low possibility of a peak signal occurrence. As a result, we'll need to figure out how to disable the PAPR signal. Finally, the GFDM signal's PAPR can be described as follows [22]:

$$PAPR(dB) = 10\log_{10}\frac{0 \le n \le N^{\max} + L_{cp} + L_f - 1^{|s(n)|^2}}{E[|s(n)|^2]} \tag{13}$$

3.1. PAPR reduction scheme using CBBO based selective level mapping in GFDM

Selective Level Mapping (SLM) lowers the likelihood of a high peak but does not eliminate it. This method was proposed by Bauml et al. (1996), who introduced the SLM scheme as one of the first probabilistic techniques that was compatible with a variety of subcarriers. Figure 2 depicts the complete process of producing GFDM signals. In this figure, the transmitter block consists of conversion of data into binary bits followed by a channel coding i.e. convolution coding suitable for noisy channel. The order bit selector is used to select the

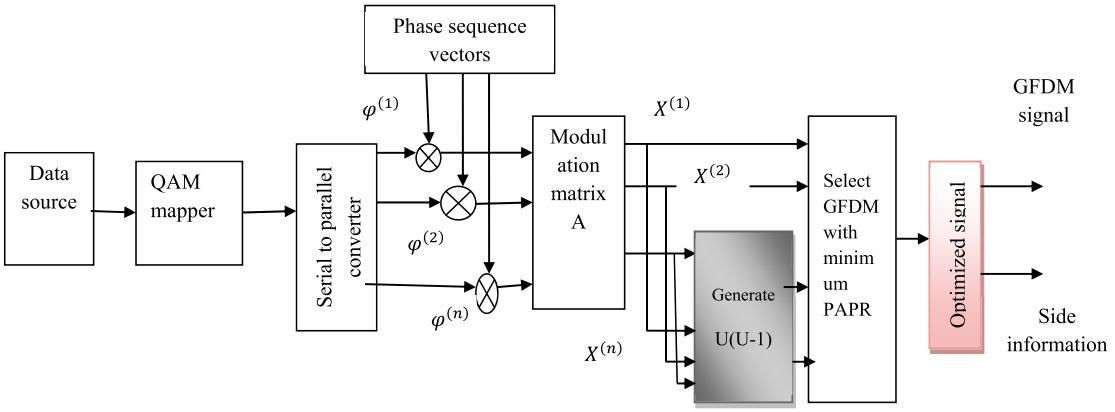

Figure 2. Block diagram of GFDM-SLM.

QAM constellation such a way that the PAPR is scaled down. The output of modulation is given as input to the serial to parallel converter, here the sub carrier is split into M non overlapping sub blocks. Then phase sequence for every sub block the GFDM signal is generated and it is applied modulaton matrix in order to minimize PAPR in the GFDM system. By using optimization algorithm the phase factors are generated. To retrieve the data at the receiver, receiver should know the generation scheme.

The input data is separated into many sub-blocks and transformed to parallel by the converter in this approach [8] is the definition of the supplied data:

$$X = [X_0, X_1, X_2, \ldots., X_{N-1}]^T \tag{14}$$

The input data sequence is then multiplied by the phase sequence to produce the input symbol sequence. Rotation factor Bv^u. rotates the phase sequence.

$$Xv^\mu = IFFT(X \otimes B^{(v\mu)}) \tag{15}$$

where

$$B^\mu = [bv_0^\mu, bv_1^\mu, bv_3^\mu, \ldots\ldots\ldots.., bv_{N-1}^\mu]^T \tag{16}$$

In the order of phases:

$$|bv_0^\mu| = 1,\ (n = 0, 1, N-1). \tag{17}$$

± 1 is commonly used to avoid the complication of complex multiplication or to combine unmodified and modified data. The supplied data is then multiplied by the phase difference U. Phase U is in the following order:

$$X^\mu = [X_0 bv_{\mu,0}, X_1 bv_{\mu,1},, X_2 bv_{\mu,2,} \ldots..X_{N-1} bv_{\mu,N-1}] \tag{18}$$

where $(\mu = 0, 1, \mathrm{U}-1)$.

Following a comparison of the U data sequences x (u), the most ideally mapped x with the lowest PAPR is chosen.

$$\hat{x} = \arg\min_{0 \le U \le U} [PAPR(X^{(v\mu)})] \tag{19}$$

To minimize the loss, use several optimization strategies in SLM by altering parameters like gain and learning rates. The CBBO is a recently proposed intelligent optimization method inspired by biogeography theory that is applied here. The biogeography-based methodology focuses mostly on examining species distribution in nearby ecosystems. Simon proposed [37] BBO after relating the phenomenon of migration and mutation during species evolution to engineering optimization challenges.

The SLM steps in the GFDM system are written in the following algorithm.

Algorithm – modelling of slm for gfdm systems

1.	$d \leftarrow b$	⊳ mapping 16 OQAM
2.	$A \leftarrow g$	⊳ pulse shaping RRC
3.	$x \leftarrow Ad$	⊳ output GFDM
4.	$X \leftarrow XN$	⊳ partition into sub block
	For n=0:N-1	
5.	$x^{vu} \leftarrow X \otimes B^{(vu)}$	⊳ multiplied with rotation factor
6.	$X^{VU} \leftarrow x^{vu}$	⊳ IFFT
7.	$PAPR(X^{VU})$	⊳ choose minimum PAPR
8.	$\tilde{x} \leftarrow$ **PAPR**(X^{VU})	⊳ optimized signal
9.	**end for**	

Chaos is a type of random motion condition that is directly derived from a deterministic equation and it is not generated by unpredictability of external causes [14]. Chaos movement's ergodicity causes the variable to traverse all states in a given range according to its laws and not to repeat. The chaos optimization technique avoids slipping into the local optimum due to the ergodicity properties of chaotic mapping, and the ability to fine search is improved.

In the BBO algorithm, the chaotic mapping operation is used to implement the selection, migration, and mutation operators. The detection capability can be improved by combining the chaotic and selection operators with the migration operator. The combination of mutation operator with chaotic strategy improves the exploring capability on the solution set. The following graph depicts the link between the habitat suitability index (HIS) and the suitability index variables (SIV).

$$HIS = f\ (Habitat) = f\ (SIV_1 - SIV_{near}) \tag{20}$$

The migration and mutation of species are important stages in BBO. The emigration rate (λ) and the

immigration rate (μ) are both functions of the population of a species (S). There are several functions that can be used to explain the relationship, but we will use the cosine model, which is shown as

$$\begin{cases} \lambda_k = \frac{I}{2}\left(1+\cos\left(\frac{k\pi}{n}\right)\right) \\ \mu_k = \frac{E}{2}\left(1-\cos\left(\frac{k\pi}{n}\right)\right) \end{cases} \tag{21}$$

When there are no species in the ecosystem, maximum immigration and zero emigration occur. As the number of species grows, the immigration rate falls to zero, whereas emigration rises to the maximum amount E. When the two rates are equal, the value of S is stabilized at one point. Assume that the species population in one habitat is λ_s, and μ_s that the immigration and emigration rates are defined as follows:

$$\lambda_s = 1(1 - {}^{S}\!/_{S_{\max}}) \tag{22}$$

$$\mu_s = {}^{ES}\!/_{S_{\max}} \tag{23}$$

Suppose that $E = I$ for simplicity, so $\lambda_s+\mu_s = E$. BBO decides whether or not to adjust SIVs based on the values of the immigration and emigration rates. The following is a detailed description of the migration procedure.

BBO updates solutions by simulating the mutation mechanism. Habitats with lower species count probability (P_S) are more prone to mutation. Assume that N is the number of habitats and that $m_{\max}$ is the maximum mutation rate. The habitat mutation rate is calculated as:

$$m(S) = m_{\max}(1 - {}^{P_S}\!/_{m_{max}}) \tag{24}$$

where $P_{\max} = \arg\max P_i$, $i = 1, 2, \ldots, N$, P_S denotes the probability that one habitats contains S kind of species. The relationship between P_S and the migration rate can be represented as:

$$P_s = \begin{cases} -(\lambda_S+\mu_S)P_s + \mu_{S+1}P_{S+1}S = 0 \\ -(\lambda_S+\mu_S)P_s + \lambda_{S-1}P_{S-1} + \mu_{S+1}P_{S+1} \\ \quad 1 \le S \le S_{\max}-1 \\ -(\lambda_S+\mu_S)P_s + \lambda_{S-1}P_{S-1}S = S_{\max} \end{cases} \tag{25}$$

Furthermore, when the population of a species in one habitat achieves a stable state, then the corresponding probability increases.

$$P_k = \begin{cases} P_0 = \frac{1}{1+\sum_{k=1}^{n}\lambda_0\lambda_1\lambda_2\lambda_3\ldots\lambda_{k-1}} k = 0 \\ P_k = \frac{\lambda_0\lambda_1\lambda_2\lambda_3\ldots\lambda_{k-1}}{1+\sum_{k=1}^{n}\frac{\lambda_0\lambda_1\lambda_2\lambda_3\ldots\lambda_{k-1}}{\mu_0\mu_1\mu_2\mu_3\ldots\mu_k}} 1 \le k \le n \end{cases} \tag{26}$$

The chaotic selection operator aids the BBO algorithm in selecting habitats in chaotic states to facilitate exploration. The chaotic migration operator, on the other hand, allows the CBBO algorithm to perform the migration operation in a chaotic pattern, restoring the exploration ability. Furthermore, in the CBBO method, distinct chaotic maps are merged with the selection operator and the migration operator to generate various exploration and exploitation patterns, enhancing the global searching ability. The random motion states obtained by constant equations are referred to as chaos. Chaotic variables exhibit chaotic states due to their randomness, ergodicity, and regularity. The term ergodicity refers to the fact that chaotic variables move through all states without repeating. Because chaotic variables are derived by constant equations, regularity implies that they are derived by constant equations. Figure 3 depicts the flow chart of CBBO-based selective level mapping in GFDM.

The common Logistic map is a typical chaotic system that is utilized with the equation as

$$Z_{n+1} = \mu Z_n(1 - Z_n);\ n = 0, 1, 2, \ldots \tag{27}$$

where μ is the control parameter and is the command parameter. This control parameter always positive and it lies in the range of $0 \le \mu \le 4$. Once the value of μ is known, the equation iterates to a fixed sequence with an arbitrary beginning value $Z_n \in [0, 1]$. When μ equals to 4, the system will be in a state of partial chaos. Because chaotic optimization is ergodic, the evolutionary process is prone to jumping out of the local optimal solution.

4. Simulation results and discussion

This section evaluates the performance of the proposed system of *SLM-based technology termed CBBO–SLM* system for the reduction of PAPR performance. The simulation was made in the in the communication environment. The modulation scheme is 16 QAM and the channel model used is AWGN. The number of subband is 8. The cyclic prefix ratio used in this work is 1/8. The parameters are summarized in Table 1.

Figure 4 displays a BER vs SNR performance experiment result for a different modulation schemes. Here QPSK and QAM modulation is used. When comparing the bit error rate (BER) performance of different digital modulation methods without taking bandwidth into account, SNR is extremely relevant. In this figure, BER

Table 1. Simulation parameter.

Number of subcarriers	$N = 128$
Type of modulation	16 QAM
Sampling frequency	15.36 MHZ
Channel model	AWGN
FFT size	1024
Type of HPA	SSPA
Oversampling factor	$L = 8$
Number of subbands	8
Cyclic prefix ratio	1/16
Length of cyclic prefix	$L_{cp} = 64$
Filter type	Dolph chebyshev
Filter length	$L_f = 64$
Search number	SN = 512

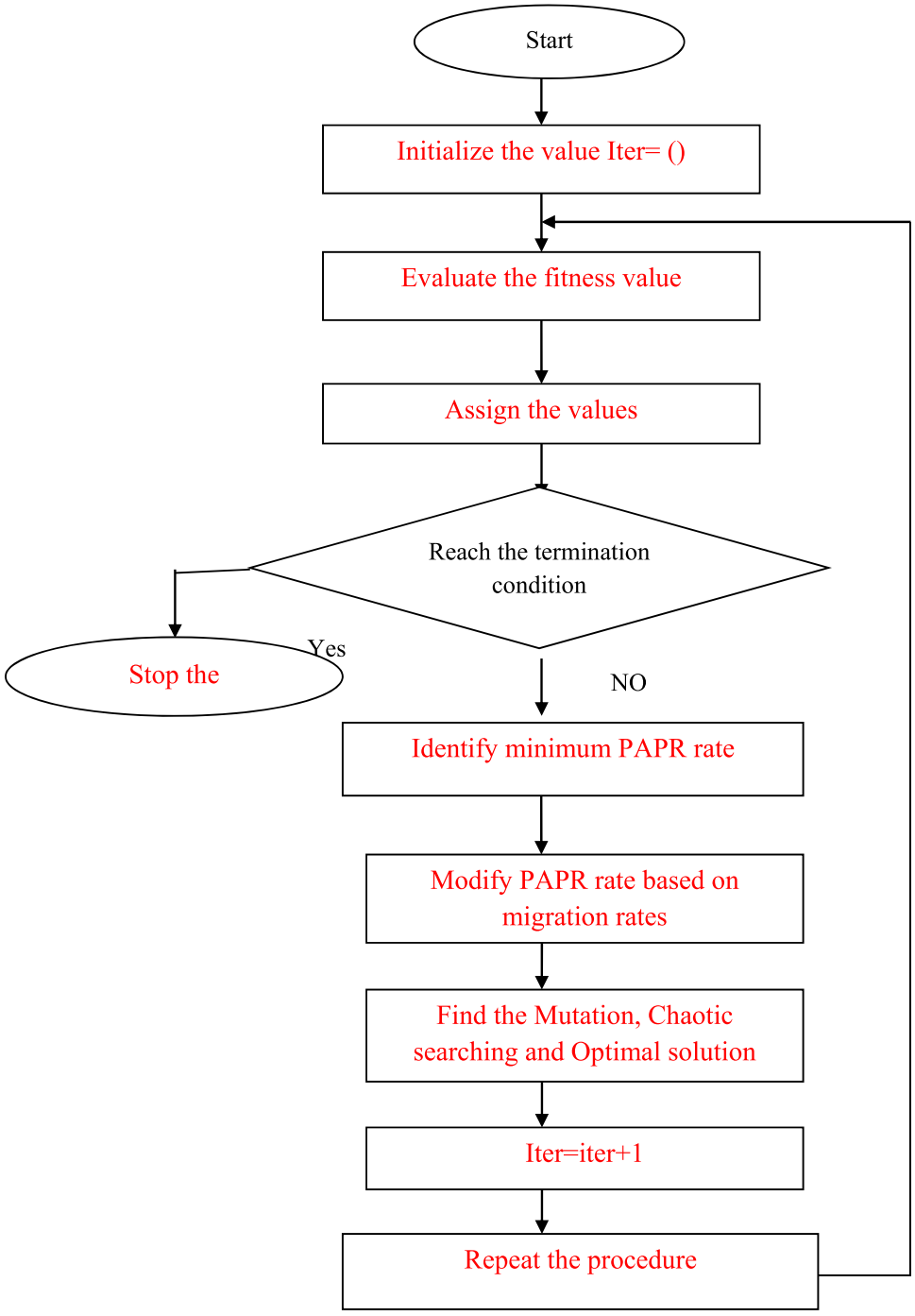

Figure 3. Flow chart of CBBO-based selective level mapping.

versus SNR for a different modulation, we note that in the QPSK modulation the SNR for BER $= 10^{-5}$ was about 14 (dB), whereas when we use QAM the results at BER $= 10^{-5}$ were 14 and 18 (dB).

QPSK is an important modulation scheme it allows for higher data rates and spectral efficiencies. It achieves high rate transmission without increasing the bandwidth in wireless communication systems. The PAPR0 [dB] – Pr [PAPR $>$ PAPR0] curve of each approach is derived in Figure 5 to evaluate the PAPR reduction capability of the CBBO–SLM method with the existing procedures. As demonstrated in Figure 5, the proposed method is obviously the best performing technique for lowering the PAPR of the original signal to the lowest values.

Even though the existing Biogeography-based SLM approaches mentioned yield some PAPR increases in specific amounts over the original signal, our proposed CBBO–SLM procedure achieves the biggest improvement. For example, for CCDF $= 10^{-5}$, the PAPR gains achieved by the GA–SLM, BBO–SLM, and CBBO–SLM over the original signal are 7, 6.50, and 5.95 dB, respectively, whereas the conventional GFDM and SLM achieve the largest gain of 11 and 7.5 dB.

The result of the subcarrier quantity on the PAPR0 [dB] – Pr [PAPR $>$ PAPR0] curves of the investigated

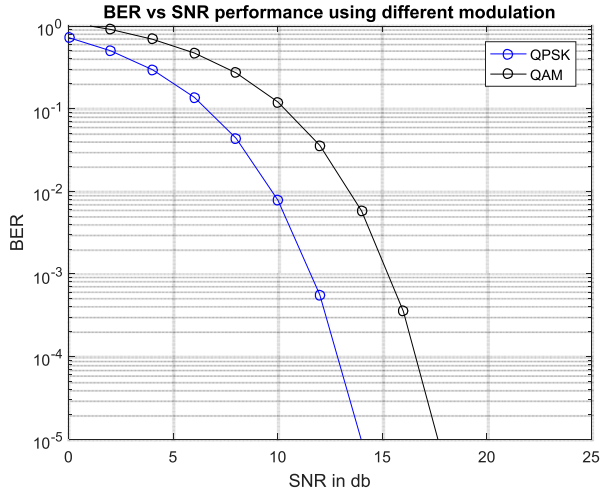

Figure 4. BER vs. SNR performances of the QPSK and QAM modulation schemes.

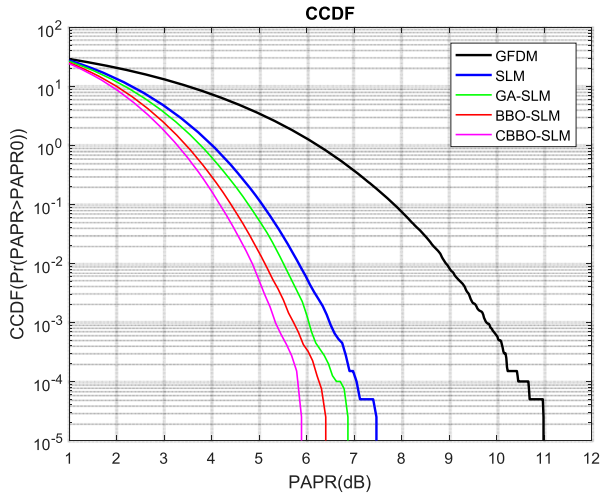

Figure 5. The effect of different parameter combinations on the PAPR reduction performance of CBBO–SLM technique.

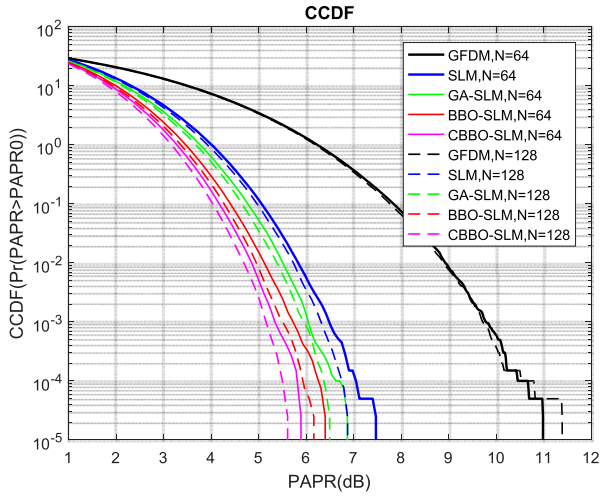

Figure 6. PAPR0 [dB] – Pr [PAPR > PAPR0] curves of the SLM, GA–SLM, BBO–SLM and CBBO–SLM schemes for 64 and 128 subcarriers.

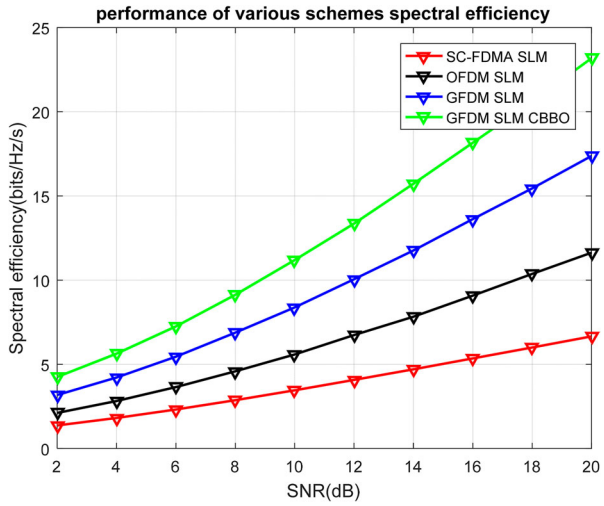

Figure 7. Spectral efficiency of the different SLM schemes.

schemes is examined in Figure 6, for 64 and 128 subcarriers respectively. In both the original and PAPR-reduced GFDM waveforms, the number of subcarriers increasing from 64 to 128 results in a certain level of PAPR growth, as shown in Figure 6. The subcarrier impact may be mathematically assessed by looking at Figure 6. While the PAPR of the original and optimized GFDM waveforms collected using the SLM, GA–SLM, BBO–SLM, and CBBO–SLM techniques is 7.5, 7.0, 6.50, 5.90, and 6.0 dB for 64 subcarriers at CCDF = 10-5, the PAPR of the related signals is 11.5, 6.95, 6.50 dB, and according to the fundamental logic, increasing the number of subcarriers in the time domain transmission signal increases the number and amplitude of higher power spikes, resulting in PAPR escalation in the linked transmission signal.

Spectral efficiency, measured in bits per second per Hz, is a valuable technique for performance analysis. Sum rate is a term used to describe spectral efficiency. The spectral efficiency of the stated PAPR reduction strategies is simulated using the parameters from Figure 7. Only Rayleigh fading is assumed in this simulation, not an AWGN channel. Less than 24fk BW is used by GFDM. Around edge subsymbol carriers have zero values due to the frequency domain RC filter. This suggests that GFDM's effective BW is less than 2M. It uses 24 subsymbol carriers with 4fM, especially in GFDM. The difference between subsymbol carriers has been extended to 4fk, and the frequency of the GFDM SLM has been widely dispersed. Spectral efficiency in wireless communications speeds is affected by the number of users accessing the network concurrently. In this scenario, the data transfer rate depends on the transmission device's bandwidth and the transmitted signal or the signal-to-noise power ratio. When the signal-to-noise ratio is improved, it also boosts spectral efficiency and channel capacity. To put it simply, more data must be sent over the available spectrum to use it efficiently.

Figure 8 illustrates the side lobe levels of the GFDM transmission signal after PAPR reduction using the SLM, GA–SLM, BBO–SLM, and CBBO–SLM

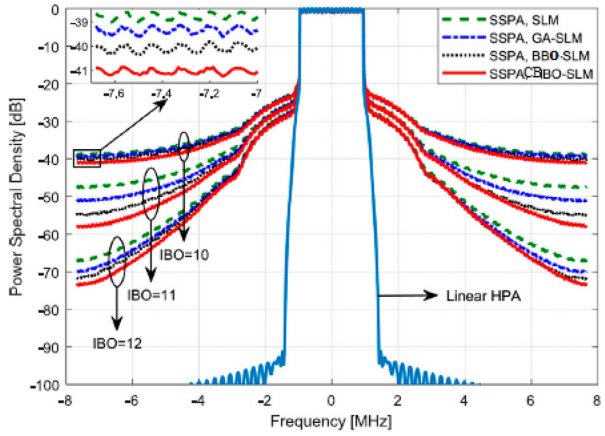

Figure 8. PSD performances of the SLM, GA–SLM, BBA–SLM and MBO–SLM schemes for varied IBOs ($p = 3$).

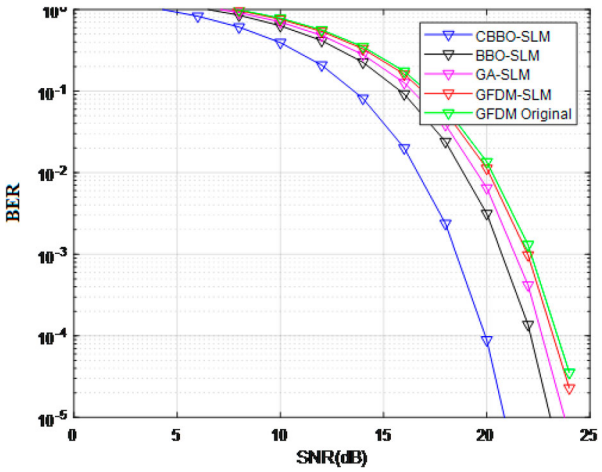

Figure 9. BER performances of the SLM, GA–SLM, BBO–SLM and CBBO–SLM for various IBO values.

techniques. In the same figure, the influence of the SSPA's input back off (IBO) parameter, which is utilized in amplifying the GFDM waveform, is evaluated for IBO values of 10, 11, and 12 dB, respectively. In this simulation, the SSPA parameter smoothness (p) is set to 3. Figure 8 clearly demonstrates the need of lowering the PAPR of GFDM waveforms via an effective approach for reducing spectral leakages by limiting the SSPA-based signal degradations found in high PAPR transmission signals. Because the CBBO–SLM method provides the greatest PAPR improvement, as demonstrated by prior simulation findings, it also produces the lowest amounts of side lobes. For IBO = 11 dB, the SLM, GA–SLM, BBO–SLM, and CBBO–SLM techniques, respectively, provide side lobe levels of −47.30 dB, −50.87 dB, −54.86 dB, and −57.60 dB. For low IBO values, SSPA amplifies the GFDM waveform close to its saturation area. SSPA is more likely to approach saturation during the amplification phase for the associated IBO values, resulting in considerable degradation of the related signals and the formation of side lobes in the PSD graph. As a consequence, raising IBO from 10 to 12 dB lowers side lobes in all of the methods depicted in Figure 8.

The first step in decreasing the BER of a GFDM waveform to acceptable levels is to minimize its high PAPR, which enhances the distortive effect of the SSPA. As shown in Figure 9, the CBBO–SLM scheme delivers the maximum BER improvement for each IBO value, because it surpasses the other strategies by lowering the PAPR of the GFDM waveform signal to the lowest level. When amplifying the original GFDM signal waveform optimized by current models and CBBO–SLM schemes, the BER values of the original GFDM signal and the corresponding PAPR reduction processes at 24 dB SNR value.

Table 2 reveals that our proposed CBBO–SLM technique beats all other strategies evaluated. The CBBO–SLM approach could be applied to a variety of transmission systems in the future to reduce PAPR. For IBO = 11 dB, the SLM, GA–SLM, BBO–SLM,

Table 2. Search complexities of the considered methods.

Author	Methods	PAPR (CCDF = 10^{-5})
Nguyen [25]	GFDM	12.5 dB
Nimir [23]	SLM	12 dB
Atul [29]	GA–SLM	11.5 dB
Necmi [38]	BBA–SLM	6.46 dB
Necmi [38]	MBO–SLM	6.30 dB
Sim [15]	BBO–SLM	6.50 dB
Proposed	CBBO–SLM	5.95 dB

and CBBO–SLM techniques, respectively, provide side lobe levels of −47.30 dB, −50.87 dB, −54.86 dB, and −57.60 dB. For low IBO values, SSPA amplifies the GFDM waveform close to its saturation area. SSPA is more likely to approach saturation during the amplification phase for the associated IBO values, resulting in considerable degradation of the related signals and the formation of side lobes in the PSD graph. As a consequence, raising IBO from 10 to 12 dB lowers side lobes in all of the methods depicted in Figure 8. In future investigations, in CA-based transmission systems, the CBBO–SLM scheme, with its great PAPR reduction capabilities, should be considered as a serious option in solving the aforementioned PAPR problem. On the other hand, comprehensive complexity analysis can reveal the practical restrictions of applying the CBBO–SLM to CA-based systems.

5. Conclusion

In this work, a unique approach was developed to provide an effective solution to the high PAPR problem of the GFDM waveform, dubbed CBBO–SLM. In a comparable method, an effective mechanism dubbed the CBBO algorithm was applied to make it acceptable for the optimization of phase sequences consisting of ones and minus ones in discrete space. The CBBO-based phase adjustment improves the performance of the SLM method. We utilized simulations to compare our suggested approach to not just classic SLM but

also state-of-the-art schemes such as GA–SLM and BBO–SLM in order to better grasp its potential. While our suggested strategy produces a total PAPR gain of 5.95 dB over the original GFDM waveform at CCDF = 10^{-5}, the CBBO–SLM technique achieves PAPR increases of 0.16, 0.30, and 0.45 dB over the BBA–SLM, GA–SLM, and conventional SLM techniques, respectively. In addition, our proposed method has the lowest BER. Simulation findings clearly demonstrate that our proposed CBBO–SLM scheme has a different potential to be among the most sought PAPR reduction techniques due to its superior performance in decreasing the PAPR of GFDM waveforms.

Disclosure statement

No potential conflict of interest was reported by the author(s).

References

[1] Kaur K, Kumar S, Baliyan A. 5G: a new era of wireless communication. Int J Inf Technol. 2020;12(2):619–624.

[2] Dragičević T, Siano P, Prabaharan SR. Future generation 5G wireless networks for smart grid: a comprehensive review. Energies. 2019;12(11):2140.

[3] Aghdam MH, Sharifi AA. PAPR reduction in OFDM systems: an efficient PTS approach based on particle swarm optimization. ICT Express. 2019;5(3):178–181.

[4] Seyyed Hadi Masoumian. Behzad Mozaffari Tazehkand. Greedy deterministic pilot pattern algorithms for OFDM sparse channel estimation. Wirel Pers Commun. 2015;84(2):1119–1132.

[5] Chen J, Wen C, Ting P. An efficient pilot design scheme for sparse channel estimation in OFDM systems. IEEE Commun Lett. 2013;17(7):1352–1355. doi:10.1109/LCOMM.2013.051313.122933.

[6] Osvaldo. Pilot-based channel estimation for OFDM by tracking the delay-subspace. IEEE. 2004;3(1).

[7] Srivastava MK, Shukla MK, Srivastava N, et al. A hybrid scheme for low PAPR in filter bank multi carrier modulation. Wirel Pers Commun. 2020;113(2):1009–1028.

[8] Duan S, Yu X, Wang R. Performance analysis on filter parameters and sub-bands distribution of universal filtered multi-carrier. Wirel Pers Commun. 2017;95(3):2359–2375.

[9] Ramavath S, Jha AV, Chandra U, et al. PAPR reduction of filter bank techniques for 5G communication systems. In: Ramjee Prasad, editor. 5G and beyond wireless systems. Aalborg, Denmark: Center for TeleInFrastruktur, Aalborg University: Springer; 2020. p. 171–189.

[10] Rosas AA, Shokair M, El-Dolil SA. Proposed optimization technique for maximization of throughput under using different multicarrier systems in cognitive radio networks. In The Proceedings of Second International Conference on Electronics Engineering, Clean Energy and Green Computing (EEECEGC); 2015. p. 25–33.

[11] Panaitopol D, Datta R, Fettweis G. Cyclostationary detection of cognitive radio systems using GFDM modulation. In: 2012 IEEE wireless communications and networking conference (WCNC). IEEE; 2012, April. p. 930–934. doi:10.1109/wcnc.2012.6214508.

[12] Zhang D, Mendes LL, Matthé M, et al. Expectation propagation for near-optimum detection of MIMO-GFDM signals. IEEE Trans Wireless Commun. 2015;15(2):1045–1062.

[13] Zewail I, Saad W, Shokair M, et al. Proposed approach based on GFDM for maximizing throughput in underlay cognitive radio network. Wireless Commun. 2016;8(9):323–328.

[14] Fettweis G, Krondorf M, Bittner S. GFDM-generalized frequency division multiplexing. In: Proc. 69th IEEE VTC Spring, Barcelona, Spain; Apr. 2009. p. 1–4.

[15] Sim ZA, Juwono FH, Reine R, et al. Performance of GFDM systems using quadratic programming pulse shaping filter design. IEEE Access. 2020;8:37134–37146.

[16] Jayati AE, Suryani T. Characteristic of HPA nonlinear distortion effects in MIMO-GFDM Systems. In 2018 International Conference on Information and Communication Technology Convergence (ICTC). IEEE; 2018. p. 379–384.

[17] Datta R, Michailow N, Lentmaier M, et al. GFDM interference cancellation for flexible cognitive radio PHY design. In: 2012 IEEE Vehicular Technology Conference (VTC Fall), Quebec City, QC, Canada; 2012. p. 1–5. DOI:10.1109/VTCFall.2012.6399031.

[18] Michailow N, Krone S, Lentmaier M, et al. Bit error rate performance of generalized frequency division multiplexing. In: Proc. 76th IEEE VTC Fall, Quebec City, QC, Canada; Sep. 2012. p. 1–5.

[19] Matth M, Michailow N, Gaspar I, et al. Influence of pulse shaping on bit error rate performance and out of band radiation of generalized frequency division multiplexing. In: 2014 IEEE International Conference on Communications Workshops (ICC); June 2014. p. 43–48.

[20] Michailow N, Matth M, Gaspar IS, et al. Generalized frequency division multiplexing for 5th generation cellular networks. IEEE Trans. Commun. Sept. 2014;62(9):3045–3061.

[21] Gaspar I, Michailow N, Navarro A, et al. Low complexity GFDM receiver based on sparse frequency domain processing. In: Proc. 77th IEEE VTC spring, Dresden, Germany; Jun. 2013. p. 1–6.

[22] Kishore V, Valluri SP, Vakamulla VM, et al. Performance analysis under double sided clipping and real time implementation of DCO-GFDM in VLC systems. J Lightwave Technol. 2020;39(1):33–41.

[23] Nimr A, Chafii M, Fettweis G. Precoded-OFDM within GFDM framework. In: 2019 IEEE 89th Vehicular Technology Conference (VTC2019-Spring). IEEE; 2019. p. 1–5.

[24] Wang Z, Mei L, Sha X, et al. BER analysis of WFRFT precoded OFDM and GFDM waveforms with an integer time offset. IEEE Trans Veh Technol. 2018;67(10):9097–9111.

[25] Duong Q, Nguyen HH. Walsh-Hadamard precoded circular filterbank multicarrier communications. In: 2017 International Conference on Recent Advances in Signal Processing, Telecommunications & Computing (SigTelCom). IEEE; 2017, p. 193–198.

[26] Wu J, Ma X, Qi X, et al. Influence of pulse shaping filters on PAPR performance of underwater 5G communication system technique: GFDM. Wirel Commun Mob Comput. 2017;2017:Article ID 4361589, 7 p.

[27] Sharifian Z, Omidi MJ, Farhang A, et al. Polynomial-based compressing and iterative expanding for PAPR reduction in GFDM. In: 2015 23rd Iranian Conference on Electrical Engineering. IEEE; 2015. p. 518–523.

[28] Yoshizawa A, Kimura R, Sawai R. A singularity-free GFDM modulation scheme with parametric shaping

filter sampling. In: 2016 IEEE 84th Vehicular Technology Conference (VTC-Fall). IEEE; 2016. p. 1–5.
[29] Sharma N, Kumar A, Magarini M, et al. Impact of CFO on low latency-enabled UAV using better than Nyquist pulse shaping in GFDM. In: 2019 IEEE 89th Vehicular Technology Conference (VTC2019-Spring). IEEE; 2019. p. 1–6.
[30] Liu K, Ge Y, Liu Y. An efficient piecewise nonlinear companding transform for PAPR reduction in UFMC systems. In: 2019 IEEE/CIC International Conference on Communications in China, ICCC, Changchun, China; 2019. p. 730–734. DOI:10.1109/ICCChina.2019.8855924.
[31] Taþpýnar N, Þimþir Þ. PAPR reduction based on partial transmit sequence technique in UFMC waveform. In: 2019 14th Iberian Conference on Information Systems and Technologies, CISTI, Coimbra, Portugal; 2019. p. 1–6, DOI:10.23919/CISTI.2019.8760726.
[32] Pamungkasari PD, Shubhi I, Juwono FH, et al. Time domain cyclic selective mapping for PAPR reduction in MIMO-OFDM systems. In: 2018 IEEE International Conference on Innovative Research and Development (ICIRD); 2018. p. 1–4. DOI:10.1109/ICIRD.2018.8376302.
[33] Pamungkasari PD, Sanada Y, Juwono FH, et al. Cyclic shift resolution effects on OFDM system employing cyclic-SLM with delayed correlation and matched filter. In: TENCON 2017 – 2017 IEEE Region 10 Conference; 2017. p. 153–157. DOI:10.1109/TENCON.2017.8227853.
[34] Prasad S, Jayabalan R. PAPR reduction in OFDM systems using modified SLM with different phase sequences. Wirel Pers Commun. 2020;110(2):913–929.
[35] Valluri S, Mani VV. A novel approach for reducing complexity in the SLM-GFDM system. Phys Commun. 2019;34:188–195.
[36] Taşpınar N, Şimşir Ş. PAPR reduction based on partial transmit sequence technique in UFMC waveform. In: 2019 14th Iberian Conference on Information Systems and Technologies, CISTI, Coimbra, Portugal; 2019. p. 1–6. DOI:10.23919/CISTI.2019.8760726.
[37] Taşpınar N, Şimşir Ş. An efficient SLM technique based on migrating birds optimization algorithm with cyclic bit flipping mechanism for PAPR reduction in UFMC waveform. Phys Commun. 2020;43:101225.
[38] Simon D. Biogeography-based optimization. IEEE Trans Evol Comput. 2008;12(6):702–713.